

## Impulsive Electron-Impact Double Ionization and the Two-Electron Momentum Density

B. El-Marji and J. P. Doering

*Department of Chemistry, Johns Hopkins University, Baltimore, Maryland 21218*

J. H. Moore

*Department of Chemistry and Biochemistry, University of Maryland, College Park, Maryland 20742*

M. A. Coplan

*Institute for Physical Science and Technology, University of Maryland, College Park, Maryland 20742*

(Received 10 February 1999)

Cross sections for electron-impact double ionization of magnesium have been measured in a triple coincidence experiment. When the momentum transfer is large, the double-ionization cross section as a function of the angle of the motion of the center of mass of the two ejected electrons closely resembles the analogous variation of the single-ionization cross section when the electron is ejected in a quasielastic binary collision. Assuming that the similarity in the shape of the cross section implies a similarity in the high-momentum-transfer ionization mechanism, atomic two-electron momentum densities have been derived from the data. Two-electron densities provide information on electron correlation in the atom.

PACS numbers: 34.80.Dp, 34.80.Pa

Electron-impact single ionization is employed to determine the momentum density of atomic and molecular electrons [1]. The purpose of the present research is to use electron-impact double ionization to obtain electron-pair momentum densities. Measured single-electron momentum densities are useful in assigning orbital symmetries and in distinguishing between alternative theoretical wave functions. The distribution of the two-electron density is the physical observable that most directly reflects electron correlation. The single-electron momentum-density research was based on detailed investigation of the kinematics of ionization that resulted in the establishment of the experimental conditions for which the target-electron momentum could be directly related to the measured cross section [2–4]. What is sought here are the conditions for which the double-ionization cross section can be related to the two-electron momentum density.

The angular distribution of ejected electrons from electron-impact single ionization is characteristic of the momentum transfer in the ionizing collision if the impact energy is more than a few times the ionization energy [5]. When the momentum transfer,  $K$ , is greater than 1 a.u., the angular distribution approaches that of hard-sphere collisions with ionized electrons preferentially ejected in the momentum-transfer direction. Ejected electrons also appear in the backward (antimomentum-transfer direction) as a consequence of backscattering from the residual ion core. These high-momentum-transfer conditions are very much different from low-momentum-transfer electron-impact ionization where the angular distribution of electrons from either single or double ionization is similar to that obtained from photoionization [5–7].

For high-momentum-transfer single ionization, a polar plot of the cross section as a function of the ejection angle relative to the incident-electron direction (an Ehrhardt

plot [5]) shows a lobe centered on the momentum transfer direction. Impulsive electron-electron collisions with the ion core participating only as a spectator account for the electrons ejected into this lobe. The shape of the lobe reflects the target-electron momentum distribution at the instant of collision. The realization of an analogous, impulsive, high-momentum-transfer, double-ionization regime from which two-electron momentum densities can be derived is the subject of this paper.

The experiments described here are completely (eightfold) differential cross section measurements of electron-impact double ionization—so-called  $(e, 3e)$  measurements. The target is magnesium, a pseudo-two-electron atom with two  $3s$  electrons outside a closed-shell doubly charged core. It is the direct ionization of the  $3s$  electrons that is being studied. A triple-coincidence measurement is carried out to measure, from each double ionization event, the ejected-electron momenta,  $\mathbf{p}_1$  and  $\mathbf{p}_2$ , and the incident and scattered electron momenta,  $\mathbf{p}_0$  and  $\mathbf{p}_s$ , from which the momentum transfer,  $\mathbf{K} = \mathbf{p}_0 - \mathbf{p}_s$ , is calculated along with the center-of-mass momentum of the two ejected electrons,  $\mathbf{P} = \mathbf{p}_1 + \mathbf{p}_2$ . To obtain momentum-transfer values in excess of 1 a.u., the kinematics are restricted to relatively high incident-electron energies and large scattering angles. In our experiments the incident energy is in the range 732 to 1032 eV and the scattering angle  $\theta_s$  is  $18^\circ$  giving values of  $|\mathbf{K}|$  in the range 2.3 to 2.7 a.u. The energies of the ejected electrons are equal:  $E_1 = E_2 = 55$  eV, well in excess of the 22 eV double ionization potential of magnesium. These ejected-electron energies correspond to momenta of magnitude  $|\mathbf{p}_1| = |\mathbf{p}_2| = 2.0$  a.u.

In double ionization, the magnitude of the ejected electrons' center-of-mass momentum is a function of the angle,  $\omega_{12}$ , between  $\mathbf{p}_1$  and  $\mathbf{p}_2$ . We observe events

for which this angle falls in the range  $91^\circ < \omega_{12} < 170^\circ$ . The corresponding magnitude of the center-of-mass momentum extends from  $|\mathbf{P}| = 0.37$  a.u. to  $|\mathbf{P}| = 2.82$  a.u., a value somewhat greater than the magnitude of the momentum transfer. Our apparatus permits a three-dimensional observation of ejected and scattered electrons. For the present experiments, the ejected-electron detectors, although arranged in a 3D array, are positioned so that  $\mathbf{p}_0$ ,  $\mathbf{p}_s$ ,  $\mathbf{K}$ , and  $\mathbf{P}$  lie in a common plane. We are thus able to display the measured cross sections as a function of the angle of orientation of  $\mathbf{P}$  in polar plots that are analogous to the Ehrhardt plots of single ionization.

The  $(e, 3e)$  cross section is small in comparison to single ionization cross sections and decreases rapidly with increasing incident energy and with increasing momentum transfer. Moreover, the statistical exigencies of triple-coincidence measurements place severe limits on the incident-beam current and target density required for optimum signal-to-noise. Of necessity,  $(e, 3e)$  spectrometers are multiplexed devices with arrays of detectors so that many triple-coincidence measurements can be carried out at the same time [8,9]. The virtue of making many simultaneous measurements is quite evident in the present experiments involving high incident-electron energies and large momentum transfers—the triple-coincidence rate for each set of three detectors is a few tens of events per week.

Our  $(e, 3e)$  apparatus has been described in detail elsewhere [9,10]; the electron optics and the magnesium-vapor source will not be specifically discussed, however, it is important to understand the detector arrangement employed in these experiments. A vector diagram of the  $(e, 3e)$  experiment is shown in Fig. 1 and superimposed on it are the apertures of the scattered-electron detector and ejected-electron detectors. The scattered-electron detector aperture is a segment of an annular aperture with a polar angle width  $\Delta\theta_s = \pm 2^\circ$  and an azimuthal

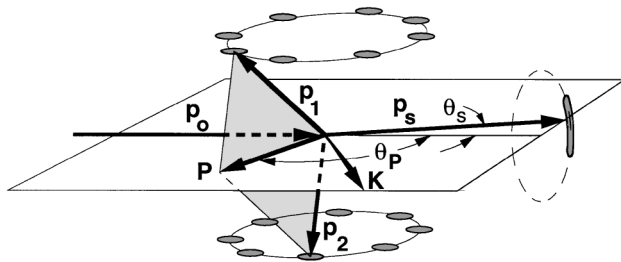


FIG. 1. A vector diagram of the  $(e, 3e)$  experiment superimposed upon a diagram showing the location and effective apertures of the scattered-electron detector and the array of ejected-electron detectors.  $\mathbf{p}_0$  and  $\mathbf{p}_s$  are the momentum vectors of the projectile electron before and after scattering,  $\mathbf{p}_1$  and  $\mathbf{p}_2$  are the momentum vectors of the ejected electrons,  $\mathbf{P}$  represents the ejected electrons' center-of-mass momentum, and  $\mathbf{K}$  the momentum transfer.

extent  $\Delta\phi_s = \pm 20^\circ$ . Sixteen ejected-electron detectors are positioned at  $45^\circ$  to a line perpendicular to the incident-electron direction with  $\pm 7^\circ$  apertures. 64 coincidence measurements are performed simultaneously, each corresponding to a triple coincidence between an electron arriving at the scattered-electron detector, an ejected electron arriving at one of the eight “upper” ejected-electron detectors, and a second ejected electron arriving at one of the eight “lower” ejected-electron detectors. The incident- and scattered-electron momentum vectors define a horizontal scattering plane as shown in the figure. The momentum transfer vector  $\mathbf{K}$  lies in this plane. With the ejected-electron detectors arranged as shown, and choosing equal energies for the ejected electrons, the ejected-electron center-of-mass momentum vector  $\mathbf{P}$  lies in the plane of  $\mathbf{p}_0$ ,  $\mathbf{p}_s$ , and  $\mathbf{K}$ .

Cross section data for the double ionization of the outer two  $3s$  electrons of magnesium by electron impact at an incident electron energy of 1032 eV are shown in Fig. 2. The cross sections are measured for eight values of  $|\mathbf{P}|$ . These data are binned in four groups with  $|\mathbf{P}| = (2.75 \text{ to } 2.82 \text{ a.u.}), (2.26 \text{ to } 2.46 \text{ a.u.}), (1.42 \text{ to } 1.73 \text{ a.u.}),$  and  $(0.37 \text{ to } 0.74 \text{ a.u.})$  and presented as polar plots of cross section as a function of  $\theta_P$ , the angle of the ejected-electron center-of-mass momentum vector,  $\mathbf{P}$ , with respect to the incident electron direction,  $\mathbf{p}_0$ . The direction and magnitude of the scattered-electron momentum and the momentum transfer are indicated. When the magnitude of  $\mathbf{P}$  is similar to that of the momentum transfer,  $\mathbf{P}$  tends to be oriented in the momentum-transfer direction. In the top panels a lobe centered on the momentum transfer direction appears that is similar in appearance to that seen for single ionization in the impulsive regime. For small values of  $|\mathbf{P}|$ , the cross sections are essentially isotropic in  $\theta_P$ .

If no momentum is transferred to the ionic core by the collision, the initial momentum of the target electrons can be determined from a measurement of their momentum following knockout from the atom. This can be demonstrated in a simple accounting for momentum conservation in a (double) ionizing collision.

The total momentum before the collision is equal to that following the collision:

$$\mathbf{p}_0 + \mathbf{p}_{\text{ion}}^i + \mathbf{q}_1 + \mathbf{q}_2 = \mathbf{p}_s + \mathbf{p}_1 + \mathbf{p}_2 + \mathbf{p}_{\text{ion}}^f, \quad (1)$$

where  $\mathbf{q}_1$  and  $\mathbf{q}_2$  are the momenta of the target electrons before the collision,  $\mathbf{p}_{\text{ion}}^i$  is the momentum of the doubly charged atomic core before the collision, and  $\mathbf{p}_{\text{ion}}^f$  is the momentum of the core after the collision. If the target atom is stationary,  $\mathbf{p}_{\text{ion}}^i + \mathbf{q}_1 + \mathbf{q}_2 = 0$ , or  $\mathbf{q}_1 + \mathbf{q}_2 = -\mathbf{p}_{\text{ion}}^i$ . In other words,  $\mathbf{p}_{\text{ion}}^i$  is the momentum with which the residual-ion core would recoil following the removal of two electrons in a collision in which the ion is a spectator. The difference between the final and initial core momenta,  $\mathbf{p}_{\text{ion}}^f - \mathbf{p}_{\text{ion}}^i$ , is the momentum imparted to the core by the collision.

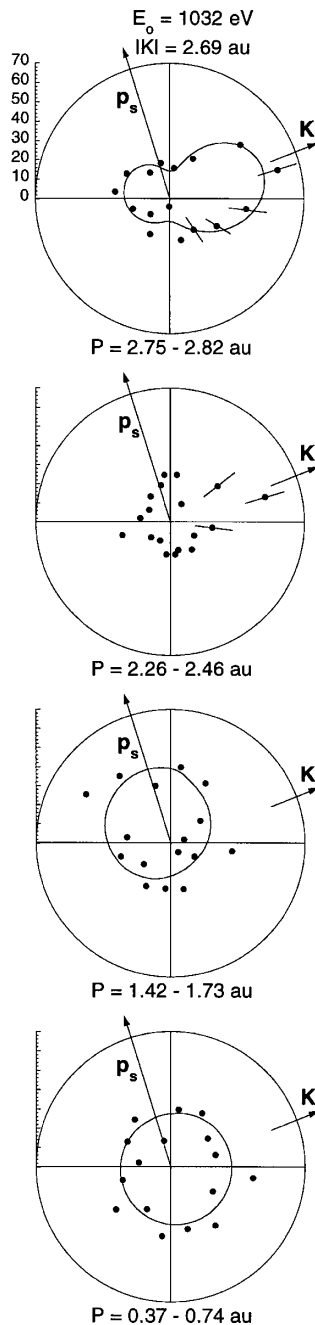


FIG. 2. Polar plots of relative cross section as a function of the angle,  $\theta_p$ , of the center-of-mass momentum of the two ejected electrons from the double ionization of the  $3s$  electrons of magnesium by electron impact at an incident-electron energy of 1032 eV with momentum transfer of 2.69 a.u. From top to bottom are shown data for which the magnitude of  $\mathbf{P}$  falls in the range (2.75 to 2.82 a.u.), (2.26 to 2.46 a.u.), (1.42 to 1.73 a.u.), and (0.37 to 0.74 a.u.). The incident-electron direction is vertically upward. The scattered-electron momentum vector,  $\mathbf{p}_s$ , and the momentum-transfer vector,  $\mathbf{K}$ , are shown to scale on each plot. The radial scale is the same on all plots and corresponds to the true triple coincidence rate per week (over a background of accidental coincidences). Error bars represent statistical uncertainty. The curves shown are polynomial fits to the data intended only to guide the eye.

For a stationary target atom, the momentum transfer is

$$\mathbf{K} = \mathbf{p}_0 - \mathbf{p}_s = \mathbf{p}_1 + \mathbf{p}_2 + \mathbf{p}_{\text{ion}}^f = \mathbf{P} + \mathbf{p}_{\text{ion}}^f. \quad (2)$$

Since  $\mathbf{K}$  and  $\mathbf{P}$  are measured in the experiment, the residual ion momentum can be determined:

$$\mathbf{p}_{\text{ion}}^f = \mathbf{K} - \mathbf{P}. \quad (3)$$

For collisions where the ion is a spectator and no momentum is imparted to the core by the incident electron,

$$\mathbf{p}_{\text{ion}}^f = \mathbf{p}_{\text{ion}}^i = -(\mathbf{q}_1 + \mathbf{q}_2) = -\mathbf{q} = \mathbf{K} - \mathbf{P}. \quad (4)$$

In this case,  $\mathbf{q}$ , the net momentum of the target pair in the atom at the moment of collision, can be determined from the measurement of  $\mathbf{K}$  and  $\mathbf{P}$ .

While single-electron momentum densities have been extensively studied in  $(e, 2e)$  experiments, only a few theoretical studies of electron pair momentum densities have been carried out [11,12] and there have been no comparable experiments. The single-electron momentum density is given directly by the impulsive  $(e, 2e)$  cross section as a function of the target electron momentum (or, equivalently, the ion recoil momentum). The analogous  $(e, 3e)$  measurement of the two-electron density requires the cross section be measured as a function of variables that depend jointly on the coordinates of two electrons. In momentum space, the coordinates for the two-electron problem have been chosen to be the relative momentum,  $\mathbf{Q} \equiv \mathbf{q}_1 - \mathbf{q}_2$ , and the net momentum,  $\mathbf{q}$ , defined above. The effect of electron correlation on the calculated two-electron density in each of these coordinates has been clearly demonstrated [11]. The relative and net momentum vectors are the obvious choice of independent variables for the experimental study of two-electron momentum densities and, as demonstrated above, it is a straightforward matter to determine  $\mathbf{q}$  in the requisite impulsive  $(e, 3e)$  measurement.

From a kinematic point of view, our experiments are analogous to the argon  $3s$  and  $3p$  single-ionization experiments of Avaldi, McCarthy, and Stefani carried out at a similar incident energy (1 keV) and over a similar range of momentum transfers (1.3 to 3.0 a.u.) [13]. The angular distributions of ejected electrons seen in these experiments display both a forward and backward lobe. The residual ion momentum for ejection in the momentum-transfer direction is just the recoil momentum and is therefore small. The cross section in the forward lobe, plotted against the residual-ion momentum, clearly reflects the momentum distribution of the target electron in the atom. For double ionization with no momentum transfer to the core, the residual-ion momentum can be anticipated to be similarly small—less than about 1 a.u. For example, the measured mean momentum of a single uncorrelated  $3s$  electron is less than 0.5 a.u. [14] and hence the mean net momentum of a pair of  $3s$  electrons will be less than 1 a.u. The available calculations

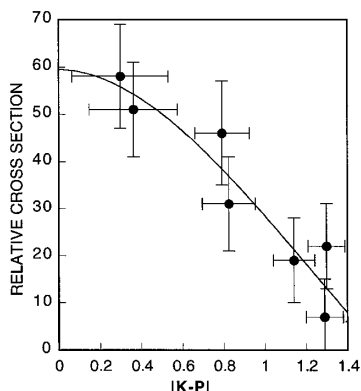


FIG. 3. The cross section for double ionization of the  $3s$  electrons of magnesium by 1032-eV electron impact in collisions for which the residual ion momentum,  $|\mathbf{p}_{\text{ion}}^f| = |\mathbf{K} - \mathbf{P}|$ , is relatively small. The vertical error bars represent the statistical uncertainty in the cross section measurement; the horizontal error bars correspond to the finite extent of the detector apertures. The curve shown is polynomial fit intended only to guide the eye.

of two-electron momentum distributions support the same conclusion. We therefore focus on doubly ionizing collisions where  $\mathbf{p}_{\text{ion}}^f$  is small.

In the top panels of Fig. 2, for the lobes centered on the momentum-transfer direction,  $\mathbf{P}$  and  $\mathbf{K}$  are of similar magnitude and oriented in roughly the same direction,  $\mathbf{p}_{\text{ion}}^f$  is small, and the condition of small momentum transfer to the core is a reasonable assumption supported by the resemblance of the large- $\mathbf{P}$  double-ionization scattering pattern to that observed in single ionization under similar conditions of high momentum transfer with the ion as a spectator. By contrast, large values of  $\mathbf{p}_{\text{ion}}^f$  correspond to  $\mathbf{P}$  opposite to  $\mathbf{K}$  (backscattering), and to small values of  $|\mathbf{P}|$  ( $\mathbf{p}_1$  opposite  $\mathbf{p}_2$ ). In Fig. 3 we have plotted the 1032-eV double-ionization cross section as a function of  $|\mathbf{K} - \mathbf{P}|$  for values of  $|\mathbf{K} - \mathbf{P}|$  less than 1.4 a.u. If one concludes that double ionization contributing to these data is the result of impulsive collisions with no involve-

ment of the ion, then the variation of the cross section with  $|\mathbf{K} - \mathbf{P}|$  is a measure of the two-electron momentum distribution of the magnesium  $3s$  electrons at the instant of knockout.

This research was supported by NSF Grant No. PHY-95-15516.

- 
- [1] M. A. Coplan, J. H. Moore, and J. P. Doering, *Rev. Mod. Phys.* **66**, 985 (1994).
  - [2] R. Camilloni, A. Giardini-Guidoni, I. E. McCarthy, and G. Stefani, *Phys. Rev. A* **17**, 1634 (1978).
  - [3] E. Weigold, C. J. Noble, S. T. Hood, and I. Fuss, *J. Phys. B* **12**, 291 (1979).
  - [4] B. Wingerden, J. T. N. van Kimman, M. Tilburg, and F. J. de Heer, *J. Phys. B* **14**, 2475 (1981).
  - [5] H. Ehrhardt, K. Jung, G. Knoth, and P. Schlemmer, *Z. Phys. D* **1**, 3 (1986).
  - [6] I. Taouil, A. Lahmam-Bennani, A. Duguet, and L. Avaldi, *Phys. Rev. Lett.* **81**, 4600 (1998).
  - [7] A. Lahmam-Bennani, I. Taouil, A. Duguet, M. Lecas, L. Avaldi, and J. Berakdar, *Phys. Rev. A* **59**, 3548 (1999).
  - [8] A. Duguet, A. Lahmam-Bennani, M. Lecas, and B. El Marji, *Rev. Sci. Instrum.* **69**, 3524 (1998).
  - [9] M. J. Ford, J. P. Doering, J. H. Moore, and M. A. Coplan, *Rev. Sci. Instrum.* **66**, 3137 (1995).
  - [10] J. H. Moore, M. A. Coplan, J. W. Cooper, J. P. Doering, and B. El Marji, in *Proceedings of the Fifteenth International Conference on the Application of Accelerators in Research and Industry*, edited by J. Duggan and I. L. Morgan, AIP Conf. Proc. No. 475 (AIP, New York, 1999).
  - [11] J. Wang and V. H. Smith, Jr., *J. Chem. Phys.* **99**, 9745 (1993).
  - [12] K. E. Banyard and R. J. Mobbs, *J. Chem. Phys.* **88**, 3788 (1988); R. J. Mobbs and K. E. Banyard, *ibid.* **78**, 6106 (1983).
  - [13] L. Avaldi, I. E. McCarthy, and G. Stefani, *J. Phys. B* **22**, 3305 (1989).
  - [14] Y. Zheng, I. E. McCarthy, E. Weigold, and D. Zhang, *Phys. Rev. Lett.* **64**, 1358 (1990).